Materials Advances

ROYAL SOCIETY OF CHEMISTRY

PAPER

View Article Online
View Journal | View Issue

Cite this: *Mater. Adv.*, 2022, 3, 8361

Strategy for optimizing the synthesis and characterization of activated carbons obtained by chemical activation of coffee husk

Alvine Mirabelle Soukoua Ngueabouo,[a] Rufis Fregue Tiegam Tagne,[ab] Donald Raoul Tchuifon Tchuifon,[ac] Cyrille Ghislain Fotsop,[d] Arnaud Kamdem Tamo[efg] and Solomon Gabche Anagho*[a]

The present work aims on the one hand to optimize the main influencing factors in the synthesis of activated carbon obtained from coffee husk as a widely available lignocellulosic precursor, and on the other hand to study its textural and chemical characteristics. The preparation methodology is done by chemical activation using phosphoric acid (H_3PO_4) and potassium hydroxide (KOH) in an atmosphere of N_2. The optimization of the main factors obtained by screening was carried out by the response surface methodology (RSM). The effects of the concentration of the activating agent, the residence time in the furnace and the carbonization temperature on the iodine number and the yield were evaluated by the ANOVA test, the Pareto diagram and the *t*-test. The optimal conditions for producing activated carbon have been recognized as being: an activation temperature of 300 °C associated with a residence time of 120 min with a concentration of 0.1 mol L^{-1} of KOH and an activation temperature of 600 °C associated with a residence time of 120 min with a concentration of 0.1 mol L^{-1} of H_3PO_4, which gave for the iodine number a value of 603.45 and 520.65 mg g^{-1} and the yield of 59.054% and 67.236% respectively for activation with KOH and H_3PO_4. The various carbons with optimal properties have undergone various physicochemical analyzes such as pH at the point of zero charge (pH_{ZPC}), Bohem titration, Fourier transform infrared spectroscopy (FTIR), X-Ray Diffraction (XRD), Brunauer–Emmett–Teller (BET) analysis, Thermogravimetric analysis (TGA) and Scanning Electron Microscopy (SEM). The analysis results obtained under these optimal conditions revealed a predominantly amorphous structure, the presence of various surface functional groups (carboxylic, lactone and phenol), a dominant acid character (1.89 and 2.28 meq g^{-1}) and an advanced development of the porosity of the activated carbon produced with a specific surface of 520.55 and 560.65 m^2 g^{-1} respectively for carbon activated with base and carbon activated with acid, indicating good candidates for the production of porous materials. The activated carbons obtained by impregnation using 0.1 M of activated KOH at a temperature of 300 °C for 120 minutes have a good affinity with respect to the diode molecules which provide information on the microporosity of the activated carbons.

Received 26th May 2022,
Accepted 26th September 2022

DOI: 10.1039/d2ma00591c

rsc.li/materials-advances

[a] *Department of Chemistry, Research Unit of Noxious Chemistry and Environmental Engineering, Faculty of Science, University of Dschang, Dschang, Cameroon. E-mail: sg_anagho@yahoo.com*
[b] *Department of Paper Sciences and Bioenergy, University Institute of Wood Technology, University of Yaoundé I, Mbalmayo P.O. Box. 306, Cameroon*
[c] *Department of Process Engineering, National Higher Polytechnic School of Douala, University of Douala, P.O. Box. 2701 Douala, Cameroon*
[d] *Institute of Chemistry, Faculty of Process and Systems Engineering, Universität Platz 2, 39106 Magdeburg, Germany*
[e] *Laboratory for Bioinspired Materials—BMBT, Institute of Microsystems Engineering—IMTEK, University of Freiburg, 79110 Freiburg, Germany*
[f] *Freiburg Materials Research Center—FMF, University of Freiburg, 79104 Freiburg, Germany*
[g] *Freiburg Center for Interactive Materials and Bioinspired Technologies—FIT, University of Freiburg, 79110 Freiburg, Germany*

1. Introduction

Activated carbon recognized as a class of porous carbonaceous materials has been the subject of several studies over the last decade in the context of environmental protection regulations.[1] Due to its high adsorption capacity, high thermal stability and ease of regeneration as well as good chemical stability, it is commonly used as an adsorbent material for industrial applications.[2–5] Recently, activated carbon has also been used as a precursor material for grafting acrylic acid polymers to inhibit shale hydration in the oil and gas industry.[6] Activated carbon is considered a material that can provide unique surface characteristics with the appropriate high pore volume.[7]

The design and operation of the activated carbon preparation process is convenient and can be handled easily, and therefore the operation costs are relatively low.[4] Many other researchers have confirmed that activated carbon is a reference material containing millions of tiny pores resulting from the activation process.[8] Lignocellulosic materials due to their low relative cost have been used as precursors in the preparation of activated carbon.[9]

Activated carbon is recognized as one of the best adsorption materials prepared from different organic substances for multiple applications such as wastewater treatment.[10] The adsorption capacity of activated carbons is mainly linked by their method of preparation (chemical or physical activation).[10] The porous structure and the adsorption properties of activated carbons are mainly obtained in carbonaceous materials by a process of chemical or physical activation.[11,12] Physical activation is a two-step process. The first step is the carbonization of the raw material.[13] The latter involves the pyrolysis of a carbonaceous material at a temperature between 600 °C and 1000 °C to reduce the elements oxygen and hydrogen. And followed by the second step, which is the activation of the carbonized material in the presence of N_2, CO_2 or high temperature steam. Physical activation does not involve any chemicals, thus reducing the cost of production.[13] In the chemical activation process, the precursor material is treated with dehydrating activating agents such as H_3PO_4, $ZnCl_2$, KOH and NaOH, before pyrolysis.[14,15] The low activation temperature and the development of pores in the carbon structure through the use of chemicals make chemical activation the most desirable method. Physical activation gives a lower yield compared to chemical activation due to oxidation of carbonaceous constituents of biomass during the carbonization and activation process.[14] Indeed, activating chemical compounds inhibit the formation of tars and volatile matter by improving the yield of activated carbon.[16] The advantage of chemical activation is that higher efficiency with larger surface area could be achieved.[14,15]

The dehydration and oxidation characteristics of the chemical activating agent require a much lower activation temperature compared to physical activation. The work of Giraldo and Ladino (2007)[17] on the comparative study of chemical and physical activation using biomass fibers reported that the surface obtained by physical activation was slightly higher than chemical activation but with lower production yield. Higher greenhouse gas emissions such as carbon monoxide and methane are produced during biomass carbonization at high temperatures, which is an unfriendly approach.[16]

One of the main factors in the production of activated carbons is the availability of precursors. Cameroon is the leading coffee producer in Central Africa.[18] This agricultural activity generates large volumes of post-harvest waste each year, creating a disposal challenge. This waste is burned in the open field, resulting in the emission of greenhouse gases responsible for air pollution and climate change. The efficient management of these wastes which contain large amounts of biopolymers such as cellulose, hemicellulose and lignin that can produce environmentally friendly and low cost adsorbents is a challenge for researchers.[19] Several published articles on activated carbon production have been made mentioning agro-waste, including cocoa pods and avocado seeds,[20–22] rice husk,[23] kenaf core fiber,[19] grape seed,[24] waste rubber tires,[7] rubber tires toward,[4] corn cob[25] and date kernel.[11] Although coffee cultivation is widely practiced around the world, to our knowledge, there are currently no published studies on the conversion of coffee husk as a lignocellulosic precursor to activated carbon.

The adsorption properties of an activated carbon are mainly influenced by preparation factors such as the concentration of the activating agent, the residence time in the furnace, the rate of impregnation and the temperature of carbonization.[26] The study of the optimization of these factors by the classical method is increasingly limited due to the large number of experiments to be carried out, which generates much higher costs and errors made during the experiments.[27] The response surface methodology appears today as the best optimization tool that studies the synergistic and antagonistic effect between several parameters on the responses with a limited number of experiments.[27,28]

Therefore, in this study is to optimize the main factors influencing the preparation of activated carbons by base (KOH) and acid (H_3PO_4) chemical activation using response surface methodology. In addition, the results of experimental conditions of the best activated carbons obtained on surface morphology, functional groups, crystallinity and thermal stability were also analyzed using SEM-EDX, FTIR, XRD and TGA respectively. The choice of coffee husk is justified by their availability and low commercial costs. This study finds its interest in the means of sustainable management of waste through the use of coffee husk as precursors of ecological and economic activated carbon. This study will also have an economic impact on Cameroon in the sense that it will reduce the importation of activated carbon from international markets.

2. Experimental

2.1. Materials

The coffee husk as a precursor were acquired from a coffee factory in Santchou which is a town in Cameroon, located in Menoua Division of the West region. These coffee husk were first dried in the sun before being washed several times with tap water and then rinsed with distilled water to get rid of all impurities. The product obtained after washing was then dried in an oven at a temperature of 90 °C until complete dehydration. After cooling, the coffee husk was stored in very dry crucibles for later use.

All chemicals (KOH, H_3PO_4, I_2, NaCl, Na_2CO_3, $NaHCO_3$, HCl, NaOH, KI) were purchased with greater than 99% purity from Merck and used as received.

2.2. Methods

2.2. 1. Synthesis of activated carbon. The activated carbons were prepared by the process of chemical activation using phosphoric acid (H_3PO_4) and potassium hydroxide (KOH) as activating agents. The different concentrations of acid and base

were prepared according to the methodology experimental plan design of experiments in the range of 0.1 to 1 mol L^{-1}. A quantity of 3 g of biomass washed and dried in an oven at 50 °C was impregnated with a solution of potassium hydroxide or orthophosphoric acid for 24 hours with stirring at a speed of 200 rpm at room temperature and at a rate impregnation of 1 : 3 (w/w), where 1 and 3 represent the mass of activating agent and raw material respectively. The mass of the dry biomass was obtained using a digital balance and that of the activating agent obtained by multiplying the density by the volume. Subsequently, the samples were filtered through filter paper and dried and kept in an oven set at 105 °C for dehydration overnight. The samples obtained were then weighed and carbonized in a Carbolite brand furnace (Model MTF 12.38.40) under an N_2 atmosphere at temperatures and residence times in the furnace given by the response surface methodology in the range of 300 at 600 °C and 30 to 120 minutes respectively.

The samples charred were then cooled in desiccators then weighed again before being washed several times with distilled water. Washing consisted of introducing the material into half a liter of water, and leaving it under stirring for 15 min, then filtered and rinsed several times until the washing water became clear, and the pH of the final washing solution was between 6 and 8 depending on the activating agent used (acidic pH for H_3PO_4 and basic for KOH). The washed samples were then dried at 105 °C in an oven for 12 hours, then ground until a particle size of less than 50 μm was obtained. The resulting activating carbon was labeled as CACA for activated carbon activated with phosphoric acid and CACB for activated carbon with potassium hydroxide. The activated carbons obtained were kept in very dry and hermetically sealed bottles while awaiting characterization.

2.2.2. Experimental design

2.2.2.1. Screening of factors. It was first a question in this part of determining the effects of the input variables on the fluctuation of the output variables in order to identify the parameters having a strong influence on the structural and textural properties of the manufactured materials commonly known under the name screening plan. Some experimental parameters often emerge from published works on the synthesis of activated carbons such as the concentration of the activating agent, the pyrolysis temperature, the rate of impregnation, the heating rate and the residence time in the furnace which are regularly cited as determining parameters of coal properties.[29] Based on this observation, the factors retained in the context of this work are, among others, the temperature varying from 300 to 600 °C; the concentration of the activating agent in the range of 0.1 to 1 M and the carbonization time in the range of 30 to 120 minutes.

2.2.2.2. Optimization by response surface methodology (RSM). The response surface methodology consists of several planes, including the Doehlert plane, the Box–Behnken plane, and the central composite design.[30] This last plan is increasingly used because it can make it possible to start a study with a minimum of experiments and to adjust if the model is not validated without however losing the results of the previous tests.[27] The central composite design is used to optimize the main influencing parameters in the preparation of activated carbons. The independent variables chosen according to the screening plan are, among others, the concentration of the activating agents, the residence time in the furnace and the carbonization temperature. By applying the Doehlert equation

$$N = 2^K + 2K + n_0 \quad (1)$$

where N is the total number of trials, K the number of factors and n_0 the number of points in the center, 17 experiments with 3 points in the center. Table 1 presents the coded variables and experimental domain which determines the limits of variation of the factors X_{min} and X_{max} within which the levels of X_1; X_2 and X_3 will be defined respectively for the calcination temperature, the concentration of the activating agent and the residence time in the furnace. The field of study is 300 X_1 600 °C; 0.1 X_2 1 mol L^{-1} and 30 X_3 120 min. The answers correspond to the quantity studied. It is also called ''objective function'' or ''response function''. The outputs correspond to the measurements of the iodine number (mg g^{-1}) Y_1 and of the yield (%) Y_2. The different responses or outputs are evaluated through a developed model correlating the response to the three factors using a second order polynomial given by quadratic equation:[31]

$$Y = \beta_0 + \sum_{i=1}^{n} \beta_i x_i + \sum_{i=1}^{n} \beta_{ii} x_i^2 + \sum_{i=1}^{n} \sum_{j=1}^{n} \beta_{ij} x_i x_j + \varepsilon \quad (2)$$

where Y represents the quantity measured; β_0 the constant of the equation, β_i the linear coefficient, β_{ii} the quadratic coefficient, β_{ij} the coefficient of the interaction, x_i and x_j the coded values of the factors and ε is the experimental error which reflects the lack of precision between two identical experiments.

Table 1 Coded and real variables

			Variables levels		
Variables	Units	Coded variables	−1	0	+1
Temperature	°C	X_I	300	450	600
Concentration	(mol L^{-1})	X_I	0.10	0.55	1
Time	(min)	X_3	30	75	120

2.2.2.3. Validation of the model. It is recommended for statistical studies to validate the empirical model obtained. Statgraphic Plus software, version 5.0 was used to analyze the experimental data. The model was accepted when the R^2 or adjusted R^2 correlation coefficient was greater than or equal to 75%. The analysis of variance (ANOVA) was used to model the responses measured by a quadratic equation of order 2. The hypothesis taken into account in this study refers to a probability of the index p less than 5%. The significant factors were evaluated by the Pareto diagram and the values of the probability p. If the t-test value is large and the p-value small, then the coefficient is more significant. The accuracy of the model was also proven by the difference between the experimental values obtained from the model with those obtained during the manipulation.

3. Physical and chemical characterization of activated carbons

The physical and chemical properties of the synthesized activated carbons were then determined as seen below.

3.1. Determination of yield of activated carbon

The determination of the yield makes it possible to estimate the mass loss during the carbonization process. It was determined according to the procedure developed by Tan *et al.* (2008).[32]

The yield was calculated as:

$$Y_2 = \frac{M_I}{M_0} \times 100 \quad (3)$$

where Y_2 is the carbon yield, M_I, the final weight of activated carbon at the end of carbonization and M_0 the initial weight of the precursors with the activating agents.

3.2. Determination of iodine number

The microporosity of the activated carbon is evaluated by determining the iodine index. It was determined according to the standards established by the American Society for Tests and Materials (ASTM) and according to the procedure described by Pongener *et al.* (2015).[33] The amount of iodine adsorbed is given by the following equation:

$$Y_1 = \frac{A - C}{A} \times \frac{V \times M}{W} \times 253.81 \quad (4)$$

where A and C are the volumes of thiosulfate solution required for the blank and sample titrations respectively; W is the weight of activated carbon; M is the concentration of iodine, 253.81 g mol^{-1} = molar weight of iodine; V, volume of iodine dosed.

3.3. Boehm titration method

The procedure established by Boehm in (1994)[34] with $NaHCO_3$, Na_2CO_3, NaOH, and HCl was used to estimate the density of acidic and basic groups present on the surface of activated carbons which consists of bringing 30 mL of $NaHCO_3$, Na_2CO_3, NaOH, and HCl into contact with 0.1 g of each activated carbon and stirring the mixture at room temperature for 24 hours. After stirring, the mixture was filtered with Whatman No. 4 filter paper, 10 mL of each filtrate was titrated with a solution of NaOH or HCl with a concentration of 0.1 mol L^{-1}, depending on the case. The equivalent point was identified by the color change of the colored indicator used. The following formula was used to calculate the number of gram equivalents of the total acid and basic functions present on the surface of our different materials.[35]

$$\eta_{eqg} = N_0V_0 - N_fV_0 \quad (5)$$

where η_{eqg} (meq g^{-1}) is the gram equivalent number that reacted and N_0V_0 and N_fV_0 is the gram equivalent number before and after the reaction.

3.4. Determination of pH and zero charge point (pH_{PZC}) of activated carbons

The pH at the point of zero charge (pH_{PZC}) was determined according to the method described by Michael *et al.* (2016).[36] It is the pH value of an aqueous solution in which the surfaces of an AC have as many positive charges as negative charges. For this purpose, eight solutions of 0.1 M NaCl with an initial pH (pH_i) varying between 2 and 9 were prepared, the pH of these solutions was adjusted by adding a solution of NaOH and/or HCl to 0, 1 M. 0.1 g of each activated carbon were then introduced into 30 mL of the different solutions and the mixtures were kept under stirring for 24 hours and at room temperature until the stabilization of the pH noted as pH_f. By drawing the graph $pH_f = f(pH_i)$, the point of zero charge (pHpcn) represented the intersection between this graph and the line with equation $Y = f(X)$ which is the bisector of the first quadrant. The pH of the different solutions was measured using an ATC-mark brand pH meter.

3.5. FTIR spectrum study

The surface chemistry of activated carbons and precursors was deduced by identifying the organic functional groups on the surface of the substrates by a Fourier transform infrared spectroscopy (Thermo Scientific Nicolet is50, USA) using the KBr method. The spectra were recorded in the mid-infrared range with a resolution of 4000 to 500 cm^{-1}.

3.6. X-Ray diffraction study

This characterization technique was carried out on the activated carbons to determine their crystalline or amorphous structures. The analysis was carried out on an X-ray diffractometer, brand (PANalytical MPD.XPert Pro diffractometer, Pays-Bas) using a Cu-Kα radiation source (λ = 0.15406 Å) under a voltage of 40 kV.

3.7. Thermogravimetric analysis (TGA)

Thermogravimetric analysis (TGA) measured the change in mass of a material as a function of temperature and time, in a controlled atmosphere. It was used in this study to evaluate the thermal stability of the samples. It was carried out on a TGA/DTA, NETZSCHSTA 409C/CD, Freiburger Material for Schungszentrum (Germany) thermo-balance under a controlled atmosphere to avoid combustion of the material.

3.8. Scanning electron microscope (SEM)

Scanning electron microscopy analysis was used to assess the microstructure of the morphological surface of activated carbon. It was carried out using the device (XL30 ESEM from FEI, Hillsboro), equipped with an energy dispersive X-ray detector (Genesis EDX, USA).

3.9. Surface area analysis (BET)

The Brunauer–Emmett–Teller (BET) method was used to determine the surface area of activated carbon under nitrogen adsorption at 77 K from isotherms. This analysis was carried

out using a sorptophotometric porosimeter (Thermo Electron Corporation Advanced Data Processing)

4. Results and discussion

4.1. Optimization by iodine number and yield using central composite design

The results of the experimental matrix of the central composite design and the response values obtained from the experimental work are presented in Tables 2 and 3 respectively for activated carbon by phosphoric acid and by potassium hydroxide.

The results of the preparation show that when the activation temperature is 300 °C, combined with a high concentration of the activating agent of 1 mol L^{-1} and a low residence time in the furnace of 30 minutes, the yields of the activated carbons increase for both acid and base used as activating agent as shown in Tables 2 and 3. It can also be seen from these tables that the increase in the calcination temperature decreases the percentage yield of activated carbon. This can be explained by the decomposition of the material by the further release of volatile matter at high temperature.[27] The works of Abechi *et al.* (2013)[37] and Juang *et al.* (2001)[38] presented similar results. Temperature and time have a negative influence on yield. This observation was also reported by studies conducted by Gueye *et al.* (2014)[39] on jatropha wood and peanut shells impregnated with phosphoric acid and potassium hydroxide.

The iodine number increases with the carbonization temperature when the activating agent is phosphoric acid and decreases with the temperature when potassium hydroxide is used as activating agents. The increase in iodine number with decreasing temperature can be explained by inferring that decreasing temperature can cause opening of pores and consequently increasing the adsorption of iodine molecules.[27,40] Thus, as the temperature decreases for the phosphoric acid activation, the decrease in iodine value could be associated with dehydration and destruction of micropores at long residence times in the oven.[41] It turns out that the concentration of the activating agent, the residence time in the furnace and the calcination temperature improve the performance of the activated carbon. Indeed, the pyrolysis temperature has a favorable influence on the adsorption properties of activated carbons, independently of the adsorbed compound (I_2). A temperature of 600 °C promotes the development of adsorption properties with the porosity of CACA. Much higher temperatures are mentioned in the literature as best for maximum porosity development. For CACB, a temperature of 300 °C was obtained as effective for the development of adsorption properties. This phenomenon explains the negative effect of temperature on the index of the diode. Indeed, some biomasses develop better porosity at lower temperatures beyond which there is contraction of the carbon network.[42] With regard to the factors concentration of the activating agent and residence time in the oven, they show positive effects on the adsorption capacity of CACA and CACB. These results indicate that the experimental range defined for these factors (0.1–1 M; 30–120 minutes), the adsorption capacity of the two activated carbons improves with the increase of these factors.

4.2. Statistical analysis

The results of the analysis of variance which was used to evaluate the effect between the different factors on the two responses are presented in Tables 4 and 5 respectively for the acid and basic activated carbons. The factors are more significant when the probability is less than or equal to 0.05% or the confidence interval is 95%.

The results show the concentration of the activating agent and the residence time in the furnace have a quadratic influence on the iodine number of the carbon obtained by acid activation. On the other hand, for carbon prepared by basic activation, the iodine number is influenced in a linear, quadratic and interactive way by the calcination temperature, the concentration of the activating agent and the residence time in

Table 2 Matrix of experimental design and results of carbon obtained by activating with phosphoric acid

Run				Y_1 (mg g^{-1})			Y_1 (%)		
No.	X_1 (°C)	X_2 (mol L^{-1})	X_3 (min)	Y_1 exp.	Y_1 pred	Residual	Y_1 exp.	Y_1 pred	Residuals
1	450 (0)	0.55 (0)	75 (0)	304.57	312.61	−8.04	54.28	53.71	0.57
2	600 (+1)	0.10 (−1)	30 (−1)	418.78	414.11	4.69	36.49	38.12	−1.64
3	300 (−1)	0.10 (−1)	120 (+1)	475.89	480.73	−4.84	51.89	51.69	0.19
4	300 (−1)	0.55 (0)	75 (0)	304.57	304.25	0.32	57.46	61.06	−3.60
5	450 (0)	0.55 (0)	30 (−1)	323.61	342.32	−18.71	59.97	59.92	0.06
6	600 (+1)	1.00 (+1)	30 (−1)	304.57	297.99	6.58	43.95	44.11	−0.15
7	450 (0)	1.00 (+1)	75 (0)	285.53	273.79	11.74	47.08	48.27	−1.19
8	450 (0)	0.55 (0)	120 (+1)	437.82	426.08	11.74	50.99	51.21	−0.22
9	450 (0)	0.10 (−1)	75 (0)	361.68	380.39	−18.71	44.96	43.93	1.03
10	450 (0)	0.55 (0)	75 (0)	323.61	312.61	10.99	53.37	53.71	−0.34
11	300 (−1)	1.00 (+1)	30 (−1)	304.57	309.419	−4.84	**60.95**	60.27	0.68
12	600 (+1)	1.00 (+1)	120 (+1)	361.68	372.23	−10.55	28.90	29.91	−1.01
13	600 (+1)	0.55 (0)	75 (0)	304.57	311.86	−7.29	43.88	40.44	3.44
14	600 (+1)	0.10 (−1)	120 (+1)	**513.96**	507.38	6.58	25.98	26.62	−0.64
15	450 (0)	0.55 (0)	75 (0)	323.61	312.61	10.99	53.81	53.71	0.10
16	300 (−1)	1.00 (+1)	120 (+1)	380.71	383.65	−2.94	56.05	54.37	1.68
17	300 (−1)	0.10 (−1)	30 (−1)	399.75	387.46	12.29	55.95	54.90	1.05

Y exp = experimental value, *Y* pred = predicted value.

Table 3 Matrix of experimental design and results of carbon obtained by activating with potassium hydroxide

Run				Y_2 (mg g^{-1})			Y_2 (%)		
No.	X_1 (°C)	X_2 (mol L^{-1})	X_3 (min)	Y_2 exp	Y_2 pred	Residual	Y_2 exp	Y_2 pred	Residual
1	450 (0)	0.55 (0)	75 (0)	399.75	398.41	1.34	47.49	47.21	0.27
2	600 (+1)	0.10 (−1)	30 (−1)	323.61	316.45	7.15	32.58	34.74	−2.16
3	300 (−1)	0.10 (−1)	120 (+1)	**609.14**	622.93	−13.79	42.81	42.80	0.01
4	300 (−1)	0.55 (0)	75 (0)	552.03	529.24	22.79	51.07	54.64	−3.57
5	450 (0)	0.55 (0)	30 (−1)	361.68	380.77	−19.09	54.14	53.36	0.78
6	600 (+1)	1.00 (+1)	30 (−1)	304.57	287.90	16.67	37.41	37.42	−0.011
7	450 (0)	1.00 (+1)	75 (0)	342.64	376.96	−34.32	40.12	41.77	−1.65
8	450 (0)	0.55 (0)	120 (+1)	513.96	506.40	7.56	43.09	43.88	−0.79
9	450 (0)	0.10 (−1)	75 (0)	437.82	415.03	22.79	39.09	37.45	1.64
10	450 (0)	0.55 (0)	75 (0)	418.78	398.41	20.38	46.67	47.21	−0.55
11	300 (−1)	1.00 (+1)	30 (−1)	532.99	525.85	7.15	**54.56**	54.12	0.44
12	600 (+1)	1.00 (+1)	120 (+1)	494.93	480.16	14.77	22.82	23.768	−0.95
13	600 (+1)	0.55 (0)	75 (0)	323.61	357.92	−34.32	39.02	35.47	3.56
14	600 (+1)	0.10 (−1)	120 (+1)	513.96	518.23	−4.27	20.71	21.15	−0.44
15	450 (0)	0.55 (0)	75 (0)	399.75	398.41	1.34	47.51	47.21	0.30
16	300 (−1)	1.00 (+1)	120 (+1)	571.07	575.34	−4.27	50.91	48.75	2.16
17	300 (−1)	0.10 (−1)	30 (−1)	552.03	563.92	−11.89	49.06	48.11	0.95

Table 4 ANOVA for iodine number and carbon yield obtained by acid activation

		Y_1 (iodine number)				Y_1' (yield)			
Source	df	SS	MS	*F*-value	*P*-value	SS	MS	*F*-value	*P*-value
X_1	1	144.94	144.94	0.58	**0.473**	1062.49	1062.49	205.12	**0.00**[a]
X_2	1	28408.60	28408.60	112.84	**0.00**[a]	46.92	46.92	9.06	**0.02**[a]
X_3	1	17537.90	17537.90	69.66	**0.00**[a]	189.34	189.34	36.55	**0.00**[a]
X_1^2	1	55.66	55.66	0.22	**0.65**	23.45	23.45	4.53	**0.07**[a]
X_1X_2	1	724.71	724.71	2.88	**0.13**	0.18	0.18	0.04	**0.86**
X_1X_3	1	0.00	0.00	0.00	**1.00**	34.42	34.42	6.65	**0.04**[a]
X_2^2	1	561.59	561.59	2.23	**0.19**	155.17	155.17	29.96	**0.00**[a]
X_2X_3	1	181.18	181.18	0.72	**0.42**	3.62	3.62	0.70	**0.43**
X_3^2	1	13729.40	13729.40	54.54	**0.00**[a]	9.23	9.23	1.78	**0.22**

R^2 = 97.60% R^2 adjusted = 94.52% R^2 = 97.83% R^2 adjusted = 95.05%. SS = sum of squares, MS = mean square. [a] Significant value.

Table 5 ANOVA for iodine number and carbon yield obtained by base activation

		Y_2 (iodine number)				Y_2 (yield)			
Source	Df	SS	MS	*F*-value	*P*-value	SS	MS	*F*-value	*P*-value
X_1	1	73376.70	73376.70	98.77	**0.00**[a]	919.02	919.02	146.09	**0.00**[a]
X_2	1	3623.54	3623.54	4.88	**0.063**[a]	46.59	46.59	7.41	**0.03**[a]
X_3	1	39460.40	39460.40	53.12	**0.00**[a]	224.78	224.78	35.73	**0.00**[a]
X_1^2	1	5468.00	5468.00	7.36	**0.03**[a]	12.50	12.50	1.99	**0.20**
X_1X_2	1	45.29	45.29	0.06	**0.81**	5.56	5.56	0.88	**0.34**
X_1X_3	1	10191.20	10191.20	13.72	**0.01**[a]	34.30	34.30	5.45	**0.05**[a]
X_2^2	1	15.60	15.59	0.02	**0.89**	154.87	154.87	24.62	**0.00**[a]
X_2X_3	1	45.29	45.29	0.06	**0.81**	0.00	0.00	0.00	**0.99**
X_3^2	1	5468.00	5468.00	7.36	**0.03**[a]	5.30	5.30	0.84	**0.39**

R^2 = 96.68%; R^2 adjusted = 92.40%; R^2 = 97.16%; R^2 adjusted = 93.51. SS = sum of squares, MS = mean square. [a] Significant value.

the furnace. Similarly, the three factors evaluated linearly, quadratically and interactively influence the yield on all the carbon prepared. The following classification is obtained according to the increasing order *F*-value as $X_3 > X_2 > X_1$ and $X_3 > X_1 > X_2$ for the iodine number of the carbon obtained respectively by the activation by the acid and by the base. This classification shows that the iodine number is strongly influenced by the length of stay in the furnace. Since the values of R^2 and adjusted R^2 of the different synthesized activated carbons extend close to unity, it can be said that the model developed is adequate to express the two measured responses as a function of the three main optimized factors.

4.3. Mathematical modeling of the responses

By replacing the coefficients resulting from the analysis of variance in eqn (2), we obtain the quadraric equations of the

models in coded values expressing the iodine number (Y_1 and Y_2) and the yield $(Y_1' + Y_2')$. Eqn (6)–(9) express the iodine value and the yield of carbons obtained respectively by activation by the acid and by the base.

$$Y_1 = 431.40 + 0.29X_1 - 116.01X_2 - 4.24X_3 - 0.00X_1^2 - 0.01X_1X_2 + 0.00X_1X_3 + 71.50X_2^2 - 0.24X_2X_3 + 0.04X_3^2 \quad (6)$$

$$Y_1' = 45.21 + 0.07X_1 + 47.63X_2 - 0.08X_3 - 0.00X_1^2 + 0.00X_1X_2 - 0.00X_1X_3 - 37.58X_2^2 - 0.03X_2X_3 + 0.000916408X_3^2 \quad (7)$$

$$Y_2 = 1284.76 - 2.79X_1 - 36.24X_2 - 4.27X_3 + 0.00X_1^2 + 0.04X_1X_2 + 0.01X_1X_3 - 11.92X_2^2 - 0.12X_2X_3 + 0.02X_3^2 \quad (8)$$

$$Y_2' = 40.91 + 0.05X_1 + 51.71X_2 - 0.07X_3 - 0.00X_1^2 - 0.01X_1X_2 - 0.00X_1X_3 - 37.54X_2^2 - 0.00X_2X_3 + 0.00X_3^2 \quad (9)$$

The negative and positive signs which precede the factors in the various quadratic equations indicate that the factors concerned have respectively antagonistic and synergistic effects on the measured response and *vice versa*.

4.4. Interactions of independent variables

The corresponding Pareto diagrams for the optimization of the three reaction variables, namely the temperature, the concentration of the activating agent and the calcination time of the two carbons are represented in Fig. 1 for the iodine number and the yield of the carbon CACB, and Fig. 2 for iodine number and yield for CACA. The curves of the three-dimensional response surfaces resulting from the interactions are shown in Fig. 3 for CACB carbon yield, Fig. 4 and 5 respectively for iodine number and carbon yield for CACA carbon. These diagrams are drawn by considering only the most important interactions of the factors having a probability P in conformity with the advanced hypothesis, namely P less than or equal to 0.005. On this basis, the results in Table 4 show that the X_1X_3 interaction is significant for yield. Table 5 indicates that X_1X_3 interaction is significant for the iodine number and X_1X_3 for the yield.

4.5. Optimal values

The optimum conditions of preparing the two activated carbons were obtained at the maximum values of the iodine number and the yield. They are presented in Table 6. The optimal parameters were then used to prepare the other two activated carbons in order to confirm the predictions of the responnse surface methodology. Slight differences between the experimental values and the predicted values were observed, which may have resulted from experimentation or reading errors made during manipulations. This confirms that the model is valid for expressing iodine number and yield.

The activated carbons thus obtained under these optimal conditions were characterized by physico-chemical and textural techniques.

5. Characterization of activated carbon

5.1. Surface chemical functions of activated carbons

The results of the concentration of the acidic and basic functional groups present on the surface of the various samples of carbon obtained by the Bohem method are presented in Table 7.

It emerges from this table that the densities of the functional groups are almost similar between the two CAs obtained namely CACB and CACA. Their total acidity is significantly

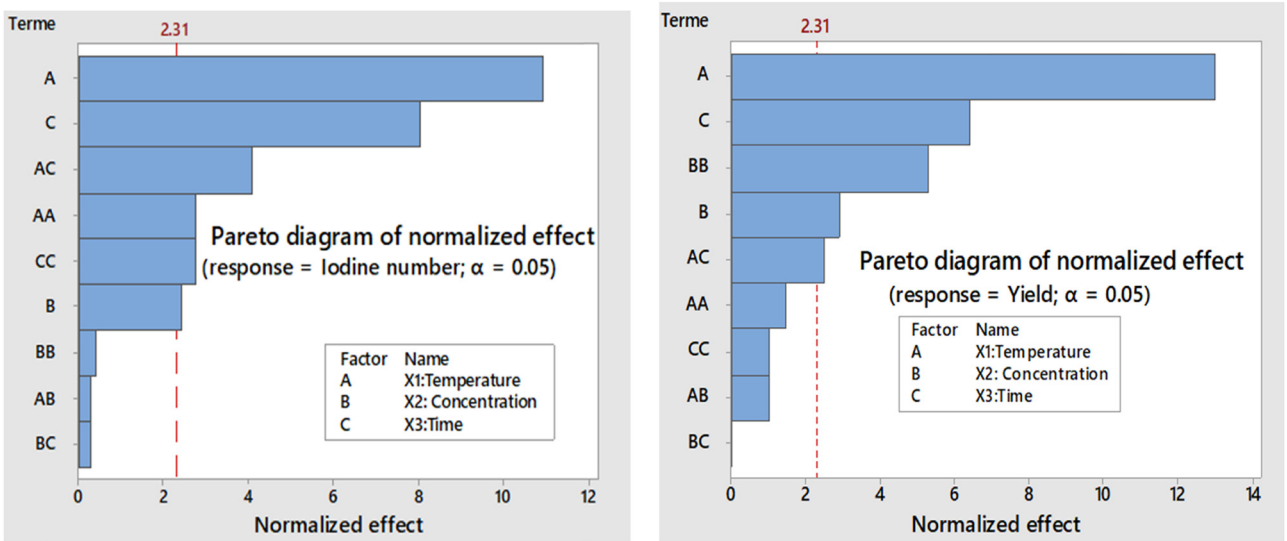

Fig. 1 Pareto chart as a function of iodine number and yield of carbon obtained by activation with base (KOH: 0.1–1 M).

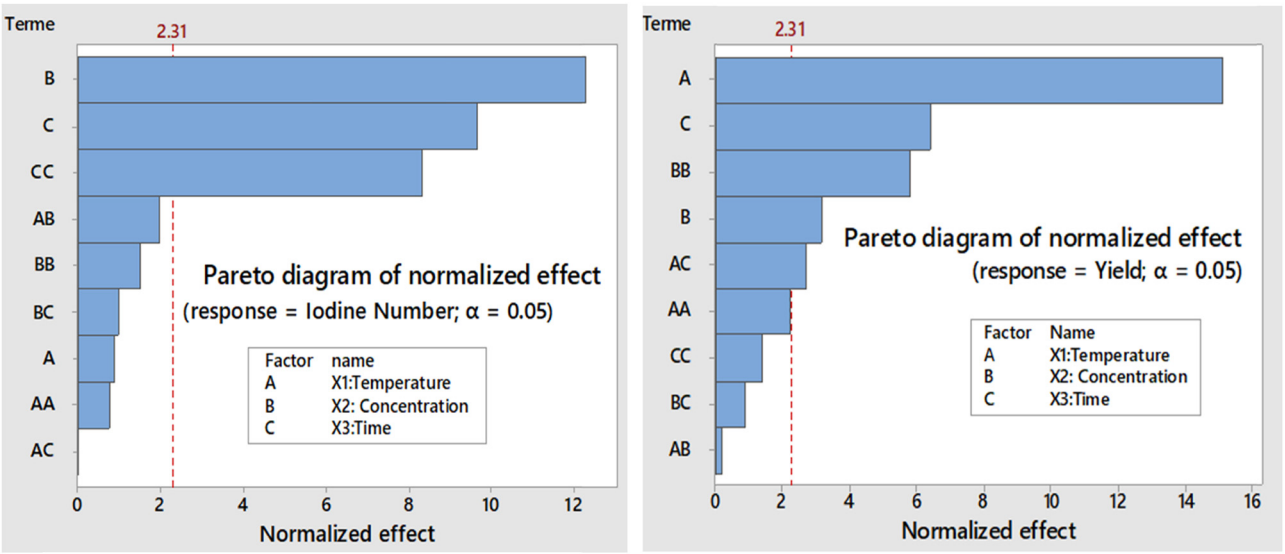

Fig. 2 Pareto chart as a function of iodine number and yield of carbon obtained by activation with acid (H_3PO_4: 0.1–1 M).

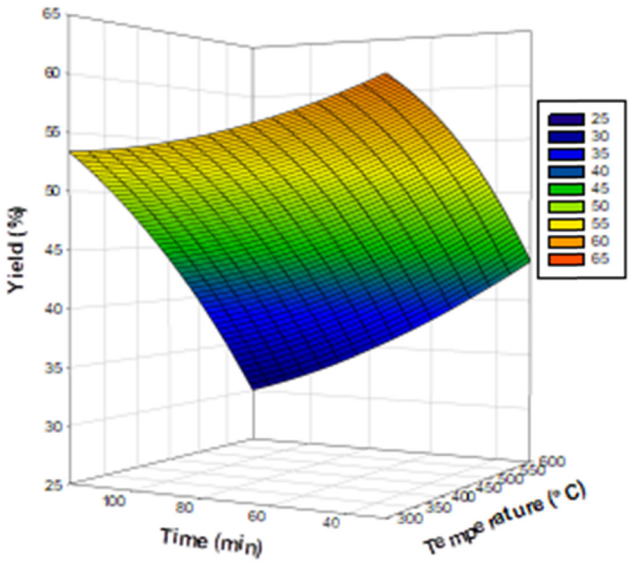

Fig. 3 Response surface diagram for the yield of activated carbon CACB obtained by activation with base as a function of the interaction, temperature–time.

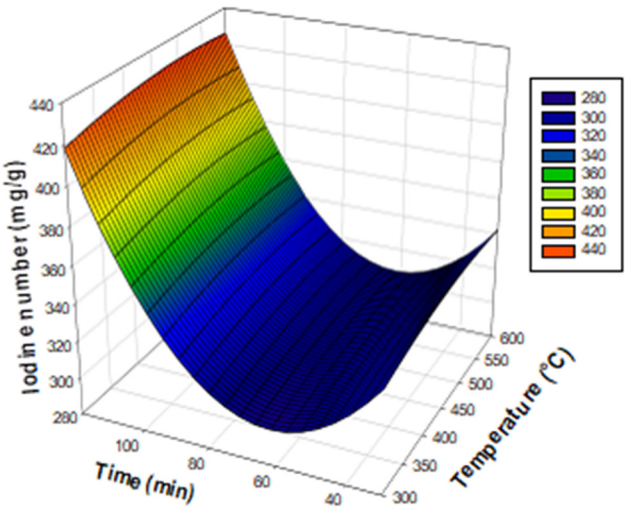

Fig. 4 Response surface diagram for the yield of activated carbon CACA, obtained by activation with acid as a function of the interaction, temperature–time.

higher than their total basicity, meaning that the prepared activated carbons have a dominant acid character. This could be explained by the fact that the activated carbons have fatty acids in their structure. On the other hand, there is a clear difference in acidity between the two activated carbons because the carbons activated with phosphoric acid H_3PO_4 have a more acidic character than those activated with potash KOH. This means that the acid and the base leave their natures on the surface of activated carbon produced during synthesis.

5.2. pH and pH_{PZC} of activated carbons

The pH_{PZC} is the pH value for which carbonaceous materials are found in their zwitterionic forms *i.e.* they carry a zero overall electronic charge. Fig. 6 illustrates the evolution of the final pH as a function of the initial pH of the activated carbons and Table 8 presents the pH and pH_{Pzc} values of the activated carbons prepared.

The results obtained show that the activated carbons prepared with the two activating agents have comparable pH values of 6.96 and 6.98. As a result these values are basic for the two activated carbons. It also emerges from this table that the pH at the point of zero charge of the synthesized carbons is of the order of 6.94 and 6.63 respectively for CACB and CACA. It is important to note that when the pH < pH_{PZC} in a solution the materials will be positively charged with the formation of the positive entity C–OH_2^+ on the surface of the materials. For values of pH > pH_{PZC} the surface of the material is charged negatively favoring the formation of negative C–O^- species on

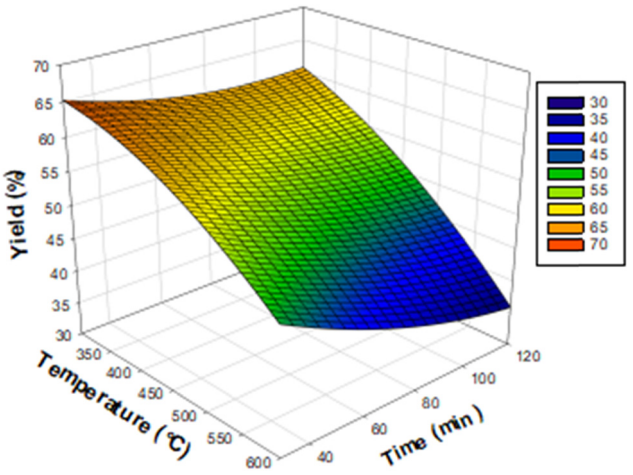

Fig. 5 Response surface diagram for the interaction temperature–time a function of the yield of carbons obtained by acid activation.

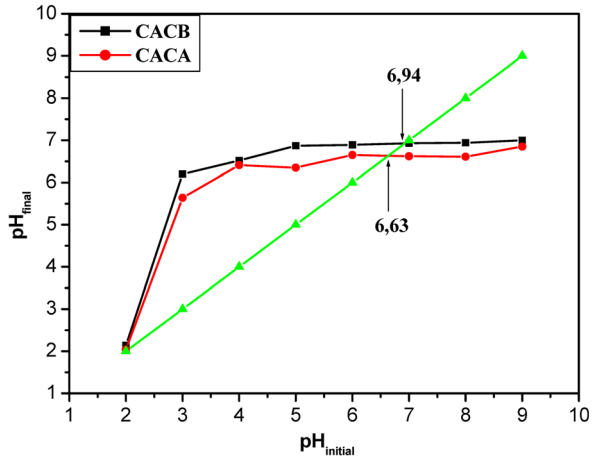

Fig. 6 Evolution of the final pH as a function of the initial pH of the activated carbons obtained on conditions: (T = 600 or 300 °C, t = 120 minutes and c = 0.1 M).

Table 6 Optimal values of the iodine number and of the yield

			IN (mg g^{-1})		
Activated Carbons	Preparation factors		Experimental values	Predicted values	Residues
CACA	X_1 (°C)	600	**520.65**	507.34	
	X_2 (mol L^{-1})	0.10			
	X_3 (min)	120			
CACB	X_1 (°C)	300	**603.45**	622.93	
	X_2 (mol L^{-1})	0.10			
	X_3 (min)	120			
Yield (%)					
CACA	X_1 (°C)	303.97	67.24	65.37	
	X_2 (mol L^{-1})	0.63			
	X_3 (min)	30.00			
CACB	X_1 (°C)	300	59.05	58.40	
	X_2 (mol L^{-1})	0.67			
	X_3 (min)	34.89			

Table 7 Concentration of surface chemical groups of the optimal activated carbons (T = 600 or 300 °C, t = 120 minutes and c = 0.1 M)

Concentration (meq g^{-1})					
Functions	Carboxylique	Lactone	Phenol	Total acidity	Total basicity
CACB	0.18	0.66	1.05	**1.89**	**0.15**
CACA	0.18	0.72	1. 38	**2.28**	**0.09**

the surface of the materials, thereby gradually decreasing the percentage of adsorption by the adsorbent due to the electrostatic repulsion between the negative charges of the solution and the surface functional groups (C–O$^-$) on the adsorbent.[43,44]

5.3. Fourier transform infrared analysis

The FTIR absorption spectra of the activated carbons and the raw material are shown in Fig. 7.

A peak is observed at about 3540–3350 cm^{-1} on the spectrum of the raw material, which may be associated antisymmetric stretching vibration –OH functional group and the C–H asymmetric stretching vibration produces a peak at 2930 cm^{-1}.[45]

Table 8 pH and pH_{PZC} values of the activated carbons prepared

Samples	CACB	CACA
pH	6.96	6.98
pH_{PZC}	6.94	6.63

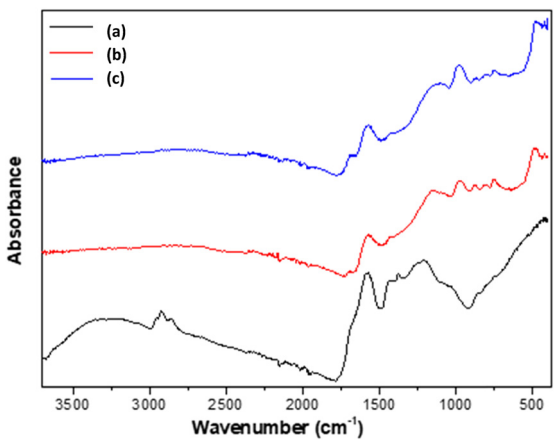

Fig. 7 IR spectra for (a) raw material (b) CACA and (c) CACB.

The intense bands at 1630 and 1550 cm^{-1} correspond respectively to stretching and aromatic skeleton vibrations C=C. We observe at 1424 and 1308 cm^{-1} bands respectively associated with C–H asymmetrical and symmetrical bending vibrations.[45] The band at 1737 cm^{-1} corresponds to the C=O stretch for carbon dioxide or carbon monoxide derivatives of the acetyl group in hemicellulose.[46] The bands visible at (1673, 1400) cm^{-1} relate to the stretching vibration of C=C aromatic compounds (in the benzene ring). The peaks observed at 1550 cm^{-1} have been attributed to the asymmetric and symmetric vibration of the N=O groups. The peak observed at 1053 cm^{-1} is associated with the antisymmetric stretching of the COC of the aromatic structure.[47] The peak detected at about 860 cm^{-1} is associated with the structure of the aromatic C–H vibrations[48] the main

oxygen groups present on the spectra of the different samples can be carbonyl, alcohol and plant cellulose groups.[49]

The spectra of CACA and CACB are different from that of the raw material by the absence of several bands that must have been lost during carbonization and activation; depending strongly on the activation temperature. The elimination of peaks at 3600 cm^{-1} on the activated carbon spectrum indicates a decomposition in oxygenated hydrocarbons of the carbohydrate structure of cellulose and

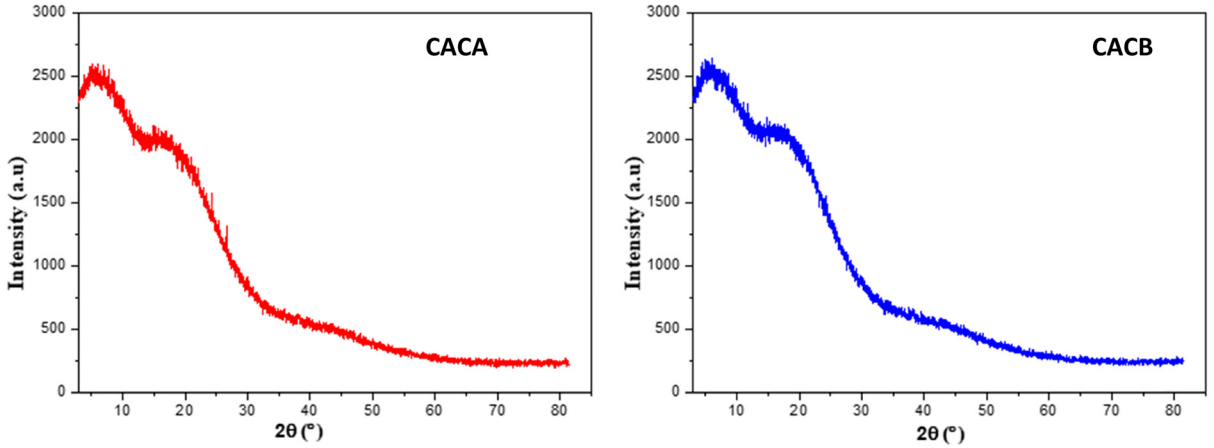

Fig. 8 XRD spectra for CACA and CACB respectively.

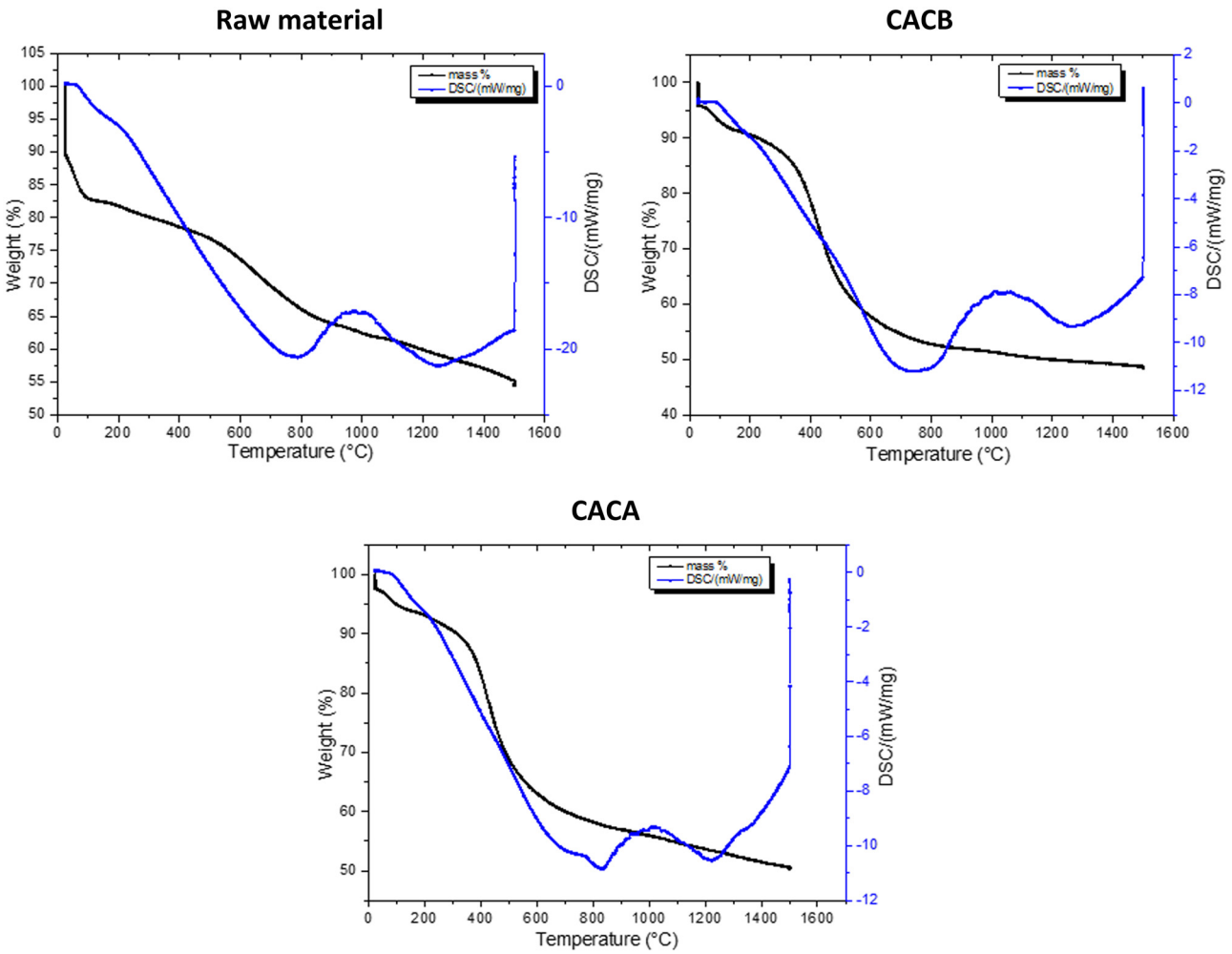

Fig. 9 Thermograms of the resulting activated carbons and the raw material.

hemicellulose.[50] It can be thought that the decrease in the intensity of the 1240 cm^{-1} band in the raw material is due to the destruction of the lignin structure containing the ester and ether bond after the chemical treatment.[51]

5.4. Phase analysis

Fig. 8 illustrates the X-ray diffraction pattern of the prepared activated carbons CACA and CACB.

The diffractogram of the two carbons shows the same appearance with two Bragg diffraction peaks respectively at $2\theta = 11^\circ$ and $2\theta = 22^\circ$ which shows the predominantly amorphous structure.[52] The existence of the bump the high degree of disorder observed on the diffractograms of carbons is a characteristic of carbonaceous materials. Similar structures have also been reported by other researchers who prepared activated carbons from different lignocellulosic raw materials.[32,33,53]

5.5. Coupled differential calorimetric and thermogravimetric analysis

This analysis was used to determine as a function of the temperature the mass losses of the functional groups contained in the various samples. The results obtained are presented in Fig. 9.

For the raw material a loss of mass is observed between 10 and 150 °C with an exothermic process as shown by the DSC curve which has an extremum at 20 °C directed towards negative values followed by an exothermic process. A significant loss is observed between 800 and 1100 °C following an endothermic process with an extremum at 1000 °C. Similar phenomena are also observed with CACA and CACB carbons, where a first loss of mass is noted in the range of 10 to 160 °C followed by another between 600 and 800 °C for the second loss and a third loss between 800 and 1200 °C. The first mass losses of the various carbons can be explained by the presence of hygroscopic molecules in recurrence of water and volatile matter.[21] The second losses may be due to carbonization which is the source of the release of carbon dioxide and carbon monoxide.[54] In view of the results it is obvious to note that these prepared materials have excellent thermal stabilities.

5.6. Surface morphology by SEM

SEM micrographs of raw materials, and the activated carbons CACA and CACB are shown in Fig. 10(a), (b) and (c) respectively.

As shown in Fig. 10(a), the surface of the raw material is curly but has no pores and no cavities. On the surface of the two activated carbons small pores are observed at an early stage of formation which could indicate the residues of tarry substances formed during the calcination stage. This observation was also confirmed by a study conducted by Thanapal *et al.* (2014)[55] which shows the surface porosity of carbonization products increase after the carbonization process resulting in surfaces with small voids. Activation with H_3PO_4 resulted in the creation of more pores on the CACA carbon surface as shown in Fig. 10(b). This variability can be explained by the diffusion of the H_3PO_4 molecule in the pores favoring the increase of the H_3PO_4-carbon reaction *via* acid hydrolysis processes which would then create more pores.[56] The results suggest that the synthesized activated carbons could have various uses due to surface porosity. In addition the SEM assisted by an electron microprobe (EDX) also allowed us to determine the majority components of CACA and CACB. The results are shown in the spectra of Fig. 11.

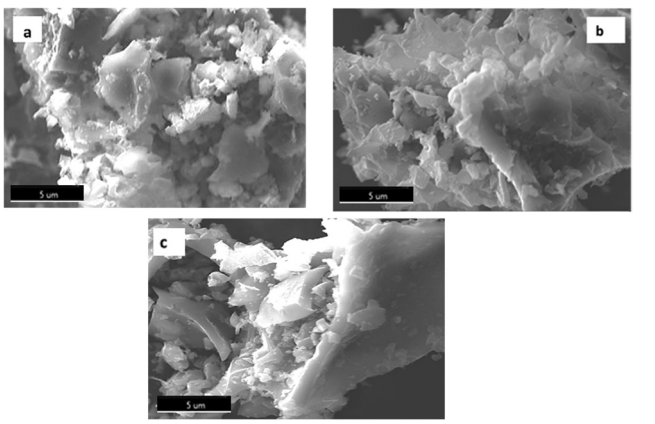

Fig. 10 Micrograph of (a) raw material. (b) CACA (activated by the H_3PO_4) and (c) CACB (activated by the KOH).

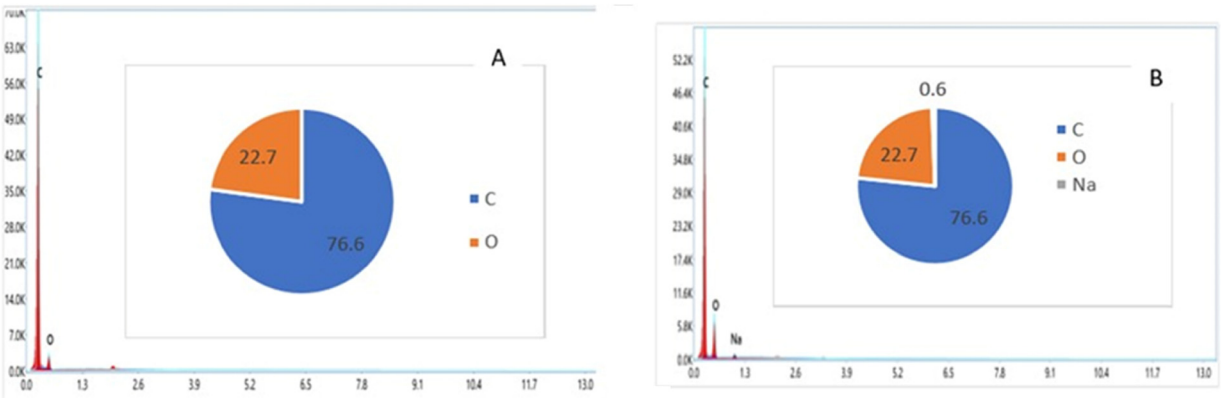

Fig. 11 Majority peaks of elements present on CACA (A) and CACB (B).

EDX analyzes of both activated carbons indicated the formation of mostly ≈77% carbon and 22% oxygen for CACA and 77% carbon and 21% oxygen with traces of sodium. The results of the spectra show that the prepared materials are dominated by carbon and oxygen. It should be noted that this probe only detects elements whose content is greater than about 0.5% and that the hydrogen content could not be determined by this technique. The high carbon content allows us to suggest that these materials could be good candidates as support materials in pollutant adsorption processes.[57]

5.7. Surface study of different activated carbons

Surface analysis by BET showed that activated carbon prepared by activation with H_3PO_4 (CACA) had better surface properties in terms of surface area with a value of 570.65 $m^2\ g^{-1}$. This could be a good indication of the use of H_3PO_4 as an activating agent for porosity development. The value of 522.55 $m^2\ g^{-1}$ was obtained for activated carbon prepared by activation with KOH (CACB). It is clearly demonstrated that the nature of the chemical activating agent influences the specific surface.[58] He demonstrated that CACA and CACB provide better carbon properties with large specific surface areas of 570.65 $m^2\ g^{-1}$ and 522.55 $m^2\ g^{-1}$ respectively.

6. Conclusion

This study consisted on the one hand in optimizing by the response surface methodology the main parameters influencing the preparation of activated carbons resulting from coffee husks using H_3PO_4 and KOH as activating agents, and on the other hand in the evaluation of performance of the best coals by various physico-chemical characterizations. The optimal conditions of concentration of the activating agent of 0.1 M for a residence time in the oven of 120 minutes and at a temperature of 600 °C and 300 °C gave respectively for CACA and CACB values in iodine number of 507, 38 mg g^{-1} and 622.93 mg g^{-1}. The experimental application of these optimal conditions gave iodine index values of 520.65 mg g^{-1} and 603.45 mg g^{-1} respectively for CACA and CACB. The difference between the theoretical value and the experimental value shows an error of 2.55% and 3.13% respectively for CACA and CACB. Physicochemical and textural characterizations were used for activated carbons prepared under optimal conditions. Boehm's titration showed a dominant acid character of the activated carbons. An SEM image indicated the surface area increase and pore development after calcination. FTIR spectroscopy showed the presence of different frequencies of the functional group. The XRD results confirmed the crystal structure and the amorphous nature of the prepared activated carbons. The BET surface of both substrates is important in surface chemistry. This study demonstrates that coffee husks could be efficient and low-cost raw materials for the preparation of highly porous activated carbons to remove organic or inorganic chemical pollutants in wastewater treatment. This result also appears as one of the solutions to the challenges faced by underdeveloped countries in general and Cameroon in particular in terms of agricultural waste recovery.

Author contributions

Conceptualization, Solomon Gabche Anagho and Rufis Fregue Tiegam Tagne; validation, Solomon Gabche Anagho and Rufis Fregue Tiegam Tagne; investigation, Alvine Mirabelle Soukoua Ngueabou, Rufis Fregue Tiegam Tagne, Donald Raoul Tchuifon Tchuifon, Cyrille Ghislain Fotsop, Arnaud Kamdem Tamo and Solomon Gabche Anagho; data curation, Alvine Mirabelle Soukoua Ngueabouo, Rufis Fregue Tiegam Tagne, Cyrille Ghislain Fotsop, and Arnaud Kamdem Tamo; writing – original draft preparation, Alvine Mirabelle Soukoua Ngueabouo and Rufis Fregue Tiegam Tagne; writing – review and editing, Solomon Gabche Anagho and Rufis Fregue Tiegam Tagne. All authors have read and agreed to the published version of the manuscript.

Conflicts of interest

The authors declare that there are no conflicts of interest.

Acknowledgements

We appreciate the technical assistance of the Researchers of Material and Process Engineering Team (MPET)/RU-NOCHEE of the Department of Chemistry. Faculty of Science. University of Dschang. Cameroon. The authors also appreciate the support of Giscard Doungmo, Institut für Anorganische Chemie, Christian-Albrechts-Universität zu Kiel, Max-Eyth-Str. 2, 24118, Kiel, 17 Germany and Dr Kuete Tiotsop Idris-Hermann from the Faculty of Science, University of Dschang, Cameroon.

References

1 J. B. Njewa, E. Vunain and T. Biswick, Synthesis and Characterization of Activated Carbons Prepared from Agro-Wastes by Chemical Activation, *J. Chem.*, 2022, 9975444, DOI: 10.1155/2022/9975444.

2 D. Prahas, Y. Kartika, N. Indraswati and S. Ismadji, Activated carbon from jackfruit peel waste by H_3PO_4 chemical activation: pore structure and surface chemistry characterization, *Chem. Eng. J.*, 2008, **140**(1–3), 32–42.

3 A. A. Ceyhan, O. Sahin, O. Baytar and C. Saka, Surface and porous characterization of activated carbon prepared from pyrolysis of biomass by two-stage procedure at low activation temperature and it's the adsorption of iodine, *J Anal Appl Pyrolysis*, 2013, **104**, 378–383.

4 N. S. Mohammad, H. R. Halim, A. Al-S. Abdulaziz, R. Mohammed and A. S. Tawfik, Kinetic and computational evaluation of activated carbon produced from rubber tires toward the adsorption of nickel in aqueous solutions, *Desalin. Water Treat.*, 2015, **5**, 17570–17578, DOI: 10.1080/19443994.2015.1086894.

5 E. M. Mistar, T. Alfatahb and M. D. Supardan, Synthesis and characterization of activated carbon from Bambusa vulgaris striata using two-step KOH activation, *j mater res technol*, 2020, **9**(3), 6278–6286.
6 A. I. Mukaila and A. S. Tawfik, Partially aminated acrylic acid grafted activated carbon as inexpensive shale hydration inhibitor, *Carbohydr. Res.*, 2020, **491**, 107960.
7 A. S. Tawfik, Simultaneous adsorptive desulfurization of diesel fuel over bimetallic nanoparticles loaded on activated carbon, *J. Cleaner Prod.*, 2017, **10**, 1–10, DOI: **10.1016/j.jclepro.2017.11.208**.
8 J. A. S. Marques, Master thesis, Royal Institute of Technology, 2013.
9 P. G. González, Activated carbon from lignocellulosics precursors: a review of the synthesis methods, characterization techniques and applications, *Renew Sust Energ Rev*, 2018, **82**(1), 1393–1414.
10 M. Mariana, E. M. Mistar, T. Alfatah and M. D. Supardan, High-porous activated carbon derived from Myristica fragrans shell using one-step KOH activation for methylene blue adsorption, *Bioresour. Technol. Rep.*, 2021, 100845, DOI: **10.1016/j.biteb.2021.100845**.
11 Z. Z. Chowdhury, S. M. Zain, R. A. Khan and S. Islam, Preparation and characterizations of activated carbon from kenaf fiber for equilibrium adsorption studies of copper from wastewater, *J. Appl. Sci., Eng. Technol.*, 2012, **29**(9), 1187–1195.
12 A. S. Tawfik, Protocols for synthesis of nanomaterials, polymers, and green materials as adsorbents for water treatment technologies, *Environ. Technol. Innovation*, 2021, **24**, 101821.
13 D. Mohammed, H. Rokiah, M. N. Mohamad and S. Othman, Characterization of physically activated acacia mangium wood –based carbon for the removal of methyl orange dye, *BioResources*, 2013, **8**(3), 4323–4339.
14 D. Mohammed, H. Rokiah, M. N. Mohamad and S. Othman, Optimization study for preparation of activated carbon from Acacia mangium wood using phosphoric acid, *Wood Sci. Technol.*, 2014, **48**(5), 1069–1083.
15 D. Mohammed, A. Tanweer, H. Rokiah, S. Norafizah, M. N. Mohamad, M. S. Junita and S. Othman, Comparison of surface properties of wood biomass activated carbons and their application against rhodamine B and methylene blue dye, *Surf. Interfaces*, 2018, **11**, 1–13, DOI: **10.1016/j.surfin.2018.02.001**.
16 H. Hadoun, Z. Sadaoui, N. Souami, D. Sahel and I. Toumert, Characterization of mesoporous carbon prepared from date stems by H_3PO_4 chemical activation, *Appl. Surf. Sci.*, 2013, **280**, 1–7.
17 L. Giraldo, Y. Ladino. Synthesis and characterization of activated carbon fibers, *Procedia Chem.*, 2007, **32**, 55–62.
18 T. Vintila, I. Ionel, R. F. T. Tiegam, A. R. Wächter, C. Julean and A. S. Gabche, Residual Biomass from Food Processing Industry in Cameroon as Feedstock for Second-generation Biofuels, *BioResources*, 2019, **14**(2), 3731–3745, DOI: **10.15376/biores.14.2.3731-3745**.
19 M. S. Shamsuddina, N. R. N. Yusoffa and M. A. Sulaimana, Synthesis and characterization of activated carbon produced from kenaf core fiber using H_3PO_4 activation, *Procedia Chem.*, 2016, **19**, 558–565.
20 T. R. F. Tagne, I. Ioana, S. G. Anagho and M. Alin-cristian, Optimization of the Activated Carbon Preparation from Avocado Seeds, Using the Response Surface Methodology, *Rev. Chim.*, 2019, **70**, 410–416, DOI: **10.37358/RC.19.2.6926**.
21 T. R. F. Tagne, T. D. R. Tchuifon, S. Remo, A. K. Nanssou, S. G. Anagho, I. Ioana and U. Sergio, Production of Activated Carbon from Cocoa Pods: Investigating Benefits and Environnemental Impacts Through Analytical Chemestry Techniques and Life Cycle Assessment, *J. Cleaner Prod.*, 2020, **20**, 0959–6526.
22 A. Tanweer and D. Mohammed, A review of avocado waste-derived adsorbents: Characterizations, adsorption characteristics, and surface mechanism, *Chemosphere*, 2022, **296**, 134036.
23 Y. Chen, S. R. Zhai, N. Liu, Y. Song, Q. D. An and X. W. Song, Dye removal of activated carbons prepared from NaOH-pretreated rice husks by lowtemperature solution-processed carbonization and H_3PO_4 activation, *Bioresour. Technol.*, 2013, **144**, 401–409.
24 M. Al Bahri, L. Calvo, M. Gilarranz and J. J. Rodriguez, Activated carbon from grape seeds upon chemical activation with phosphoric acid: Application to the adsorption of diuron from water, *Chem. Eng. J.*, 2012, **203**, 348–356.
25 E. M. Cuerda-correa, A. Macı and A. L. Ortiz, Textural and morphological study of activated carbon fibers prepared from kenaf Author' s personal copy, *Microporous Mesoporous Mater.*, 2008, **111**, 523–529.
26 Z. YAhya, A. Qodah and C. W. Z. Ngah, Agricultural biowaste materials as potential sustainable precursors used for activated carbon production: A review, *Renewable Sustainable Energy Rev.*, 2015, **46**, 218–235.
27 T. R. F. Tagne, T. R. C. Temgoua, S. A. Ngueabouo, A. N. G. Ndifor, T. D. R. Tchuifon, S. G. Anagho and T. Vintila, Development of an electroanalytical method using activated rice husk-derived carbon for the detection of a paraquat herbicide, *Carbon Trends*, 2021, **4**, 100060.
28 D. Mohammed, P. Zhou, Z. Lou, A. Tanweer, M. Shahnaz, N. A. Y. Ahmad, K. Ahmad and H. P. S. A. Khalil, Preparation and characterization of banana trunk activated carbon using H3PO4 activation: A rotatable central composite design approach, *Mater. Chem. Phys.*, 2022, **282**, 125989.
29 T. R. F. Tagne, I. Ioana, N. Adina and S. G. Anagho. Optimization of the activated carbon synthesis of peanut shells, applying surface methodology, in: Proceedings of the 27th European Biomass and Exhibition, 27–30, Lisbon Portugal, 2019, pp. 1849–1855.
30 J. Goupy. Plans d'expériences: Techniques Ingénieur, *Surface functional groups on acid-activated nutshell carbons*, ed. C. A. Toles, W. E. Marshall, and M. M. Johns, Carbon, 2006, vol. 37, pp. 1207–1214.
31 D. Sibiescu and I. Cretescu Pareto, Chart for iodine number, *Rev. Chem.*, 2015, **67**, 136–137.

32 I. A. W. Tan, A. L. Ahmad and B. H. Hameed, Preparation of activated carbon from coconut husk: Optimization study on removal of 2,4,6-trichlorophenol using response surface methodology, *J. Hazard. Mater.*, 2008, **153**(1-2), 709–717.

33 C. Pongener, D. Kibami and R. Goswamee, Synthesis and characterization of activated carbon from the biowaste of the plant Manihot esculenta, *Chem. Sci. Trans.*, 2015, **1**(4), 59–68.

34 H. P. Boehm, Some aspects of the surface chemistry of carbon blacks and other carbons, *Carbon*, 1994, **32**, 759–769, DOI: 10.1016/0008-6223(94)90031-0.

35 S. D. B. Maazou, H. I. Hima and M. Mousbahou, Elimination du chrome par du charbon actif élaboré et caractérisé à partir de la coque du noyau de Balanites aegyptiaca, *Int. J. Biol. Chem. Sci.*, 2017, **11**, 3050–3065.

36 K. Michael, V. Miyittah, W. Francis, K. K. Tsyawo, C. D. Kumah and J. E. Rechcigl, Suitability of Two Methods for Determination of Point of Zero Charge (PZC) of Adsorbents in Soils, *Commun. Soil Sci. Plant Anal.*, 2016, **47**(1), 101–111.

37 S. E. Abechi, C. E. Gimba, A. Uzairu and Y. A. Dallatu, Preparation and characterization of activated carbon from palm kernel shell by chemical activation, *Res. J. Chem. Sci.*, 2013, **3**(7), 54–61.

38 C. Juang, Hsein, J. Tao, A. D. Ronald and L. Der-Her, Assessing Probabilistic Methods for Liquefaction Potential Evaluation—An Update. International Conferences on Recent Advances in Geotechnical Earthquake Engineering and Soil Dynamics, Clemson University, 2001.

39 M. Gueye, Y. Richardson, F. T. Kafack and J. Blin, High efficiency activated carbons from African biomass residues for the removal of chromium (VI) from wastewater, *J. Environ. Chem. Eng.*, 2014, **2**, 273–281.

40 I. Demiral, A. C. Şamdan and H. Demiral, Production and Characterization of Activated Carbons from Pumpkin Seed Shell by Chemical Activation with $ZnCl_2$, *Desalin. Water Treat.*, 2016, **57**, 2446–2454.

41 D. Pertiwi, N. Yanti and R. Taslim, High potential of yellow potato (Solanum Tuberosum L.) peel waste as porous carbon source for supercapacitor electrodes, *J. Phys.: Conf. Ser.*, 2022, **2193**(1), 012019.

42 G. Mbaye, *Development of activated carbons from linocellulosic biomass for applications in water treatment*, Doctoral thesis, International Institute for Water and the Environment, 2015.

43 A. Kaveh, G. A. Behdad and H. A. K. Amirhossein, Equilibrium and kinetic adsorption study of the removal of orange-g dye using carbon mesoporous material, *J. Inorg. Mater.*, 2012, **27**, 660–667.

44 K. Malwade, D. Lataye, V. Mhaisalkar, S. Kurwadkar and D. Ramirez, Adsorption of hexavalent chromium onto activated carbon derived from Leucaena leucocephala waste sawdust: kinetics, equilibrium and thermodynamics, *Int. J. Environ. Sci. Technol.*, 2016, **13**(9), 2107–2116.

45 T. A. Saleh, Simultaneous adsorptive desulfurization of diesel fuel over bimetallic nanoparticles loaded on activated carbon, *J. Cleaner Prod.*, 2017, **10**, 1–10, DOI: 10.1016/j.jclepro.2017.11.208.

46 M. Jonoobi, J. Harun, A. Shakeri, M. Misra and K. Oksmand, Chemical composition, crystallinity, and thermal degradation of bleached and unbleached kenaf bast (Hibiscus cannabinus) pulp and nanofibers, *BioResources*, 2009, **4**(2), 626–639.

47 S. Yorgun and D. Yildiz, Preparation and characterization of activated carbons from Paulownia wood by chemical activation with H_3PO_4, *J. Taiwan Inst. Chem. Eng.*, 2015, **53**, 122–131.

48 J. Yang and K. Qiu, Preparation of activated carbons from walnut shells via vacuum chemical activation and their application for methylene blue removal, *Chem. Eng. J.*, 2010, **165**(1), 209–317.

49 S. M. Yakout and G. Sharaf El-Deen, Characterization of activated carbon prepared by phosphoric acid activation of olive stones, *Arabian J. Chem.*, 2011, **3**(2), 526–540.

50 N. S. Nasri and H. Basri, A. Garba. Synthesis and characterization of low-cost porous carbon from palm oil shell via K_2CO_3 chemical activation process, *Appl. Mech. Mater.*, 2015, **735**, 36–40.

51 T. Khadiran, M. Z. Hussein, Z. Zainal and R. Rusli, Textural and Chemical Properties of Activated Carbon Prepared from Tropical Peat Soil by Chemical Activation Method, *Bioresources*, 2015, **10**, 986–1000.

52 Z. Xu, J. Chen, X. Zhang, Q. Song, J. Wu and L. Ding, *et al.*, Template-free preparation of nitrogendoped activated carbon with porous architecture for high-performance supercapacitors, *Microporous Mesoporous Mater.*, 2019, **276**, 280–391.

53 E. M. Mistar, S. Ahmad, A. Muslim, T. Alfatah and M. D. Supardan, Preparation and characterization of a high surface area of activated carbon from Bambusa vulgaris–Effect of NaOH activation and pyrolysis temperature, *IOP Conf. Ser.: Mater. Sci. Eng.*, 2018, **334**, 0120.

54 P. Chubaakum, K. Daniel, S. Kaza, B. Rao, L. Rajib, G. Goswamee and S. Dipak, Synthesis and Characterization of Activated Carbon from the Biowaste of the Plant Manihot Esculenta, *Chem. Sci. Trans.*, 2015, **4**, 59–68.

55 S. S. Thanapal, W. Chen, K. Annamalai, N. Carlin, R. J. Ansley and D. Ranjan, Carbon Dioxide Torrefaction of Woody Biomass, *Energy Fuels*, 2014, **28**(2), 1147–1157.

56 B. Hong, G. Xue, L. Weng and X. Guo, Pretreatment of moso bamboo with dilute phosphoric acid, *BioResources*, 2012, **7**(4), 4902–4913.

57 H. Gharib and A. Ouederni, Transformation du grignon d'olive tunisien en charbon actif par voie chimique à l'acide phosphorique, *Recents Prog. Genie Procedes*, 2005, **635**, 38–45.

58 S. Bhati, J. S. Mahur, S. Dixit and O. N. Chobey, Study on effect of chemical impregnation on the surface and porous characteristics of activated carbon fabric prepared from viscose rayon, *Carbon Lett.*, 2014, **15**(1), 45–49.